

**Power-law persistence and trends in the atmosphere: A detailed study of long temperature records**J. F. Eichner,<sup>1,2</sup> E. Koscielny-Bunde,<sup>1,3</sup> A. Bunde,<sup>1</sup> S. Havlin,<sup>2</sup> and H.-J. Schellnhuber<sup>4</sup><sup>1</sup>*Institut für Theoretische Physik III, Universität Giessen, D-35392 Giessen, Germany*<sup>2</sup>*Minerva Center and Department of Physics, Bar Ilan University, Ramat-Gan, Israel*<sup>3</sup>*Potsdam Institute for Climate Research, D-14412 Potsdam, Germany*<sup>4</sup>*Tyndall Centre for Climate Change Research, University of East Anglia, Norwich NR4 7TJ, United Kingdom*

(Received 12 December 2002; published 28 October 2003)

We use several variants of the detrended fluctuation analysis to study the appearance of long-term persistence in temperature records, obtained at 95 stations all over the globe. Our results basically confirm earlier studies. We find that the persistence, characterized by the correlation  $C(s)$  of temperature variations separated by  $s$  days, decays for large  $s$  as a power law,  $C(s) \sim s^{-\gamma}$ . For continental stations, including stations along the coastlines, we find that  $\gamma$  is always close to 0.7. For stations on islands, we find that  $\gamma$  ranges between 0.3 and 0.7, with a maximum at  $\gamma=0.4$ . This is consistent with earlier studies of the persistence in sea surface temperature records where  $\gamma$  is close to 0.4. In all cases, the exponent  $\gamma$  does not depend on the distance of the stations to the continental coastlines. By varying the degree of detrending in the fluctuation analysis we obtain also information about trends in the temperature records.

DOI: 10.1103/PhysRevE.68.046133

PACS number(s): 89.75.Da, 92.60.Wc, 05.45.Tp

**I. INTRODUCTION**

The persistence of weather states on short terms is a well-known phenomenon: A warm day is more likely to be followed by a warm day than by a cold day and vice versa. The trivial forecast, that the weather of tomorrow is the same as the weather of today, was in previous times often used as a “minimum skill” forecast for assessing the usefulness of short-term weather forecasts. The typical time scale for weather changes is about 1 week, a time period that corresponds to the average duration of so-called “general weather regimes” or “Grosswetterlagen,” so this type of short-term persistence usually stops after about 1 week. On larger scales, other types of persistence occur. One of them is related to circulation patterns associated with blocking [1]. A blocking situation occurs when a very stable high pressure system is established over a particular region and remains in place for several weeks. As a result the weather in the region of the high remains fairly persistent throughout this period. It has been argued recently [2] that this short-term persistence regime may be linked to solar flare intermittency. Furthermore, transient low pressure systems are deflected around the blocking high so that the region downstream of the high experiences a larger than usual number of storms. On even longer terms, a source for weather persistence might be slowly varying external (boundary) forcing such as sea surface temperatures and anomaly patterns. On the scale of months to seasons, one of the most pronounced phenomena is the El Niño southern oscillation event which occurs every 3–5 years and which strongly affects the weather over the tropical Pacific as well as over North America [3].

The question is, *how* the persistence that might be generated by very different mechanisms on different time scales decays with time  $s$ . The answer to this question is not easy. Correlations, and in particular long-term correlations, can be masked by trends that are generated, e.g., by the well-known urban warming. Even uncorrelated data in the presence of long-term trends may look like correlated ones, and, on the

other hand, long-term correlated data may look like uncorrelated data influenced by a trend.

Therefore, in order to distinguish between trends and correlations one needs methods that can systematically eliminate trends. Those methods are available now: both wavelet techniques (WT) (see, e.g., Refs. [4–7]) and detrended fluctuation analysis (DFA) (see, e.g., Refs. [8–11]) can systematically eliminate trends in the data and thus reveal intrinsic dynamical properties such as distributions, scaling and long-range correlations very often masked by nonstationarities.

In a previous study [12], we have used DFA and WT to study temperature correlations in different climatic zones on the globe. The analysis focused on 14 continental stations, several of them were located along coastlines. The results indicated that the temperature variations are long-range power-law correlated above some crossover time that is of the order of 10 days. Above the crossover time, the persistence, characterized by the autocorrelation  $C(s)$  of temperature variations separated by  $s$  days, decayed as

$$C(s) \sim s^{-\gamma}, \quad (1)$$

where, most interestingly, the exponent  $\gamma$  had roughly the same value  $\gamma \approx 0.7$  for all continental records. Equation (1) can be used as a test bed for global climate models [13].

More recently, DFA was applied to study temperature correlations in the sea surface temperatures [14]. It was found that the temperature autocorrelation function  $C(s)$  again decayed by a power law, but with an exponent  $\gamma$  close to 0.4, pointing towards a stronger persistence in the oceans than in the continents.

In this paper, we considerably extend our previous analysis to study systematically temperature records of 95 stations. Most of them are on the continents, and several of them are on islands. Our results are actually in line with both earlier papers and in agreement with conclusions drawn from independent type of analysis by several groups [15–17]. We find that the continental records, including those on coastlines,

show power-law persistence with  $\gamma$  close to 0.7, while the island records show power-law correlations with  $\gamma$  around 0.4. By comparing different orders of DFA that differ in the way trends are eliminated, we could also study the presence of trends in the records that lead to a warming of the atmosphere. We find that pronounced trends occur mainly at big cities and can be probably attributed to urban growth. Trends that cannot be attributed to urban growth occur in half of the island stations considered and on summit stations in the Alps. A majority of the stations showed no indications of trends.

The article is organized as follows. In Sec. II, we describe the detrending analysis used in this paper, the DFA. In Sec. III, we present the result of this analysis. Sec. IV concludes the paper with a discussion.

## II. THE METHODS OF ANALYSIS

Consider a record  $T_i$ , where the index  $i$  counts the days in the record,  $i=1,2,\dots,N$ . The  $T_i$  represent the maximum daily temperature, measured at a certain meteorological station. For eliminating the periodic seasonal trends, we concentrate on the departures of  $T_i$ ,  $\Delta T_i = T_i - \bar{T}_i$ , from their mean daily value  $\bar{T}_i$  for each calendar date  $i$ , say, 2nd of March, which has been obtained by averaging over all years in the record.

Quantitatively, correlations between two  $\Delta T_i$  values separated by  $n$  days are defined by the (auto) correlation function

$$C(n) \equiv \langle \Delta T_i \Delta T_{i+n} \rangle = \frac{1}{N-n} \sum_{i=1}^{N-n} \Delta T_i \Delta T_{i+n}. \quad (2)$$

If  $\Delta T_i$  are uncorrelated,  $C(n)$  is zero for  $n$  positive. If correlations exist up to a certain number of days  $n_\times$ , the correlation function will be positive up to  $n_\times$  and vanish above  $n_\times$ . A direct calculation of  $C(n)$  is hindered by the level of noise present in the finite records, and by possible nonstationarities in the data.

To reduce the noise we do not calculate  $C(n)$  directly, but instead study the ‘‘profile’’

$$Y_m = \sum_{i=1}^m \Delta T_i.$$

We can consider the profile  $Y_m$  as the position of a random walker on a linear chain after  $m$  steps. The random walker starts at the origin and performs, in the  $i$ th step, a jump of length  $\Delta T_i$  to the right, if  $\Delta T_i$  is positive, and to the left, if  $\Delta T_i$  is negative. The fluctuations  $F^2(s)$  of the profile, in a given time window of size  $s$ , are related to the correlation function  $C(s)$ . For the relevant case (1) of long-range power-law correlations,  $C(s) \sim s^{-\gamma}$ ,  $0 < \gamma < 1$ , the mean-square fluctuations  $F^2(s)$ , obtained by averaging over many time windows of size  $s$  (see below) asymptotically increase by a power law [18]:

$$\overline{F^2(s)} \sim s^{2\alpha}, \quad \alpha = 1 - \gamma/2. \quad (3)$$

For uncorrelated data (as well as for correlations decaying faster than  $1/s$ ), we have  $\alpha=1/2$ .

For the analysis of the fluctuations, we employ a hierarchy of methods that differ in the way the fluctuations are measured and possible trends are eliminated (for a detailed description of the methods we refer to Ref. [10]).

(i) In the simplest type of fluctuation analysis (DFA0) (where trends are not going to be eliminated), we determine in each window the mean value of the profile. The variance of the profile from this constant value represents the square of the fluctuations in each window.

(ii) In the *first-order* detrended fluctuation analysis (DFA1), we determine in each window the best linear fit of the profile. The variance of the profile from this straight line represents the square of the fluctuations in each window.

(iii) In general, in the  $n$ th order DFA (DFAn) we determine in each window the best  $n$ th order polynomial fit of the profile. The variance of the profile from these best  $n$ th-order polynomials represents the square of the fluctuations in each window.

By definition, DFA0 does not eliminate trends, while DFAn eliminates trends of order  $n$  in the profile and  $n-1$  in the original time series. Thus, from the comparison of fluctuation functions  $F(s)$  obtained from different methods one can learn about both, long-term correlations and the influence of trends.

The DFA method is analogous to wavelet techniques that also eliminate polynomial trends systematically. For a detailed review of the method, see Refs. [6,7]. The conventional techniques such as the direct evaluation of  $C(n)$ , the rescaled range analysis ( $R/S$ ) introduced by Hurst (for a review, see, e.g., Ref. [19]), or the power spectrum method [16,17,20,21] can only be applied on stationary records. In the presence of trends they may overestimate the long-term persistence exponent. The  $R/S$  method is somewhat similar to the DFA0 analysis.

## III. ANALYSIS OF TEMPERATURE RECORDS

Figure 1 shows the results of the DFA analysis of the daily temperatures (maximum or mean values)  $T_i$  of the following weather stations (the length of the records is written within the parentheses): (a) Vienna (A, 125 yr), (b) Perm (RUS, 113 yr), (c) Charleston (USA, 127 yr), and (d) Pusan (KOR, 91 yr). Vienna and Perm have continental climate, while Charleston and Pusan are close to coastlines.

In the log-log plots the DFA1–3 curves are (except at small  $s$  values) approximately straight lines. For both the stations inside the continents and along coastlines the slope is  $\alpha \approx 0.65$ . There exists a natural crossover (above the DFA crossovers at very small times) that can be best estimated from DFA0 [22]. As can be verified easily, the crossover occurs roughly at  $s_\times = 10$  days, which is the order of magnitude for a typical Grosswetterlage. Above  $s_\times$ , there exists long-range persistence expressed by the power-law decay of the correlation function with an exponent  $\gamma = 2 - 2\alpha \approx 0.7$ .

Figure 2 shows the results of the DFA analysis of the daily temperatures for two island stations: Wrangelja and Campbell Islands. Wrangelja Island is a large island between the

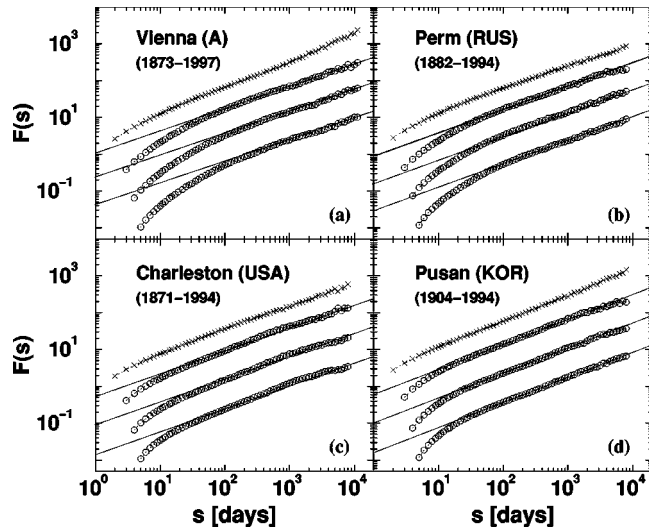


FIG. 1. Analysis of daily temperature records of four representative weather stations on continents. The four figures show the fluctuation functions obtained by DFA0, DFA1, DFA2, and DFA3 (from top to bottom) for the four sets of data. The slopes are  $0.64 \pm 0.02$  (Vienna),  $0.62 \pm 0.02$  (Perm),  $0.63 \pm 0.02$  (Charleston), and  $0.67 \pm 0.02$  (Pusan). Lines with these slopes are plotted in the figures. The scale of the fluctuation functions is arbitrary.

East Siberian Sea and the Chukchi Sea. During the winter season, large parts of the water surrounding the island are usually frozen. Campbell Island is a small island belonging to New Zealand. Again, in the double logarithmic presentation, all DFA1–3 fluctuation functions are straight lines, but the slopes differ. While for Wrangelja the slope is 0.65, similar to the land stations shown before, the slope for Campbell Island is significantly larger, close to 0.8 (corresponding to  $\gamma=0.4$ ).

It can be seen from Figs. 1 and 2 that sometimes the DFA0 curves have a larger slope than the DFA1–3 curves, and that usually the curves of DFA2 and DFA3 have the same slope for large  $s$  values. The fact that the DFA0 curve has a higher exponent indicates the existence of trends by which the long-term correlations are masked. Calculations using DFA0 alone will yield a higher correlation exponent and thus lead to a spurious overestimation of the long-term persistence. The fact that the DFA2 and DFA3 curves show

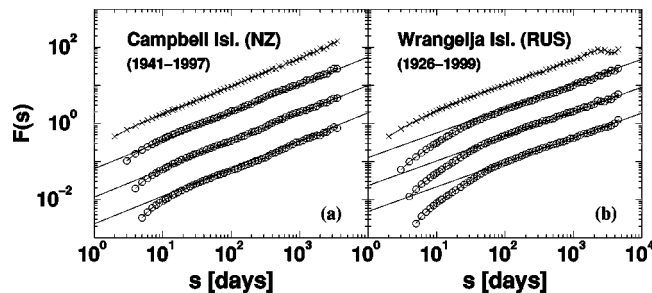


FIG. 2. Analysis of daily temperature records of two representative weather stations on islands. The DFA curves are arranged as in Fig. 1. The slopes are  $0.71 \pm 0.02$  (Campbell) and  $0.65 \pm 0.02$  (Wrangelja). Lines with these slopes are plotted in the figures.

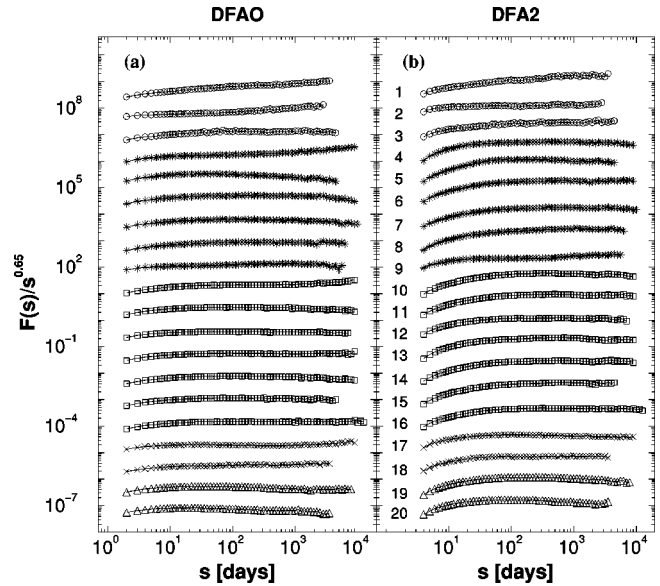


FIG. 3. Fluctuation analysis by DFA0 and DFA2 of daily temperature records of 20 representative weather stations: (1) Thursday Island (AUS, 53 yr), (2) Koror Island (USA, 54 yr), (3) Raoul Island (USA, 54 yr), (4) Hong Kong (C, 111 yr), (5) Anadir (RUS, 101 yr), (6) Hamburg (D, 107 yr), (7) Plymouth (GB, 122 yr), (8) Feodosija (UA, 113 yr), (9) Wellington (NZ, 67 yr), (10) Jena (D, 175 yr), (11) Brno (CZ, 128 yr), (12) Chita (RUS, 114 yr), (13) Tashkent (USB, 119 yr), (14) Potsdam (D, 115 yr), (15) Minsk (WY, 113 yr), (16) Oxford (GB, 155 yr), (17) Cheyenne (USA, 123 yr), (18) Kunming (C, 49 yr), (19) Wuxiaoling (C, 40 yr), (20) Zugspitze (D, 98 yr). Stations 1–3 are on islands, stations 4–9 are on coast lines, and stations 10–20 are inland stations, among them two stations (19 and 20) are on summits. The scales are arbitrary. To reveal that the exponents  $\alpha$  are close to 0.65, we have divided the fluctuation functions by  $s^{0.65}$ .

the same asymptotic behavior indicates that possible nonlinearities in the trends are not significant. Otherwise the DFA2 curve (where only linear trends are eliminated) would show an asymptotic behavior different from DFA3.

By comparing the DFA0 curves with the DFA2 curves, we can learn more about possible trends. Usually the effect of trends is seen as a crossover in the DFA0 curve. Below the crossover, the slopes of DFA0 and DFA2 are roughly the same, while above the crossover the DFA0 curve bends up. Large trends are characterized by a short crossovertime  $s_{\times}$  and a large difference in the slopes between DFA0 and DFA2 (for a general discussion see Refs. [10] and [11]). A nice example for this represents Vienna, where the DFA0 curve shows a pronounced crossover at about 3 yr. Above this crossover, the DFA0 curve bends up considerably, with an effective slope close to 0.8. For Pusan, the trend is less pronounced, and for Perm, Charleston, and the two islands we do not see indications of trends.

To reveal the presence of long-term correlations and to point out possible trends, we have plotted in Fig. 3(a) the DFA0 curves and in Fig. 3(b) the DFA2 curves for 20 representative stations around the globe. For convenience, the fluctuation functions have been divided by  $s^{0.65}$ . We do not show results for those stations that were analyzed in Ref.



value of the exponent is close to 0.65, in agreement with earlier calculations based on different methods [12,15–17].

(ii) On islands, the exponent shows a broader distribution, varying from 0.65 to 0.85, with an average value close to 0.8. This finding is in qualitative agreement with the results of a recent analysis of sea surface temperature records, where also long-term persistence with an average exponent close to 0.8 has been found [14]. Since the oceans cover more than 2/3 of the globe, one may expect that also the mean global temperature is characterized by long-term persistence, with an exponent close to 0.8.

(iii) In the vast majority of stations we did not see indications for a global warming of the atmosphere. Exceptions are mountain stations in the Alps [Zugspitze (D), Säntis (CH), and Sonnblick (A)], where urban warming can be excluded. Also, in half of the islands we studied, we found pronounced trends that most probably cannot be attributed to urban warming. Most of the continental stations where we observed significant trends are large cities where probably the fast urban growth in the last century gave rise to temperature increases.

When analyzing warming phenomena in the atmosphere, it is essential to employ methods that can distinguish, in a systematic way, between trends and long-term correlations—in contradistinction to a number of conventional schemes that have been applied in the past. These schemes run the risk of mixing up the correlatedness of natural climate system variability with entire regime shifts enforced by anthropogenic interference through greenhouse gas emissions. The fact that we found it difficult to discern warming trends at many stations that are not located in rapidly developing urban areas may indicate that the actual increase in global temperature caused by anthropogenic perturbation is less pronounced than estimated in the last IPCC (Intergovernmental Panel for Climate Change) report [24].

#### ACKNOWLEDGMENTS

We are grateful to Professor S. Brenner for very useful discussions. We would like to acknowledge financial support by the Deutsche Forschungsgemeinschaft and the Israel Science Foundation.

- 
- [1] J.G. Charney and J. Devore, *J. Atmos. Sci.* **36**, 1205 (1979).  
 [2] N. Scafetta and B.J. West, *Phys. Rev. Lett.* **90**, 248701 (2003).  
 [3] *The Science of Disasters*, edited by A. Bunde, J. Kropp, and H.-J. Schellnhuber (Springer, New York, 2002).  
 [4] *Wavelets: Theory and Applications*, edited by G. Erlebacher, M.Y. Hussaini, and L.M. Jameson (Oxford University Press, Oxford, 1996).  
 [5] M. Holschneider, *Wavelets: An Analysis Tool* (Oxford University Press, Oxford, 1996).  
 [6] A. Arneodo, Y. d'Aubenton-Carafa, E. Bacry, P.V. Graves, J.F. Muzy, and C. Thermes, *Physica D* **96**, 291 (1996).  
 [7] A. Arneodo, B. Audit, N. Decoster, J.F. Muzy, and C. Vaillant, in *The Science of Disasters* (Ref. [3]), p. 28.  
 [8] C.-K. Peng, S.V. Buldyrev, S. Havlin, M. Simons, H.E. Stanley, and A.L. Goldberger, *Phys. Rev. E* **49**, 1685 (1994).  
 [9] A. Bunde, S. Havlin, J.W. Kantelhardt, T. Penzel, J.H. Peter, and K. Voigt, *Phys. Rev. Lett.* **85**, 3736 (2000).  
 [10] J.W. Kantelhardt, E. Koscielny-Bunde, H.A. Rego, S. Havlin, and A. Bunde, *Physica A* **295**, 441 (2001).  
 [11] K. Hu, P.Ch. Ivanov, Z. Chen, P. Carpena, and H.E. Stanley, *Phys. Rev. E* **64**, 011114 (2001).  
 [12] E. Koscielny-Bunde, A. Bunde, S. Havlin, H.E. Roman, Y. Goldreich, and H.-J. Schellnhuber, *Phys. Rev. Lett.* **81**, 729 (1998).  
 [13] R.B. Govindan, D. Vyushin, A. Bunde, S. Brenner, S. Havlin, and H.-J. Schellnhuber, *Phys. Rev. Lett.* **89**, 028501 (2002).  
 [14] R.A. Monetti, S. Havlin, and A. Bunde, *Physica A* **320**, 581 (2003).  
 [15] E. Koscielny-Bunde, A. Bunde, S. Havlin, and Y. Goldreich, *Physica A* **231**, 393 (1996).  
 [16] J.D. Pelletier and D.L. Turcotte, *J. Hydrol.* **203**, 198 (1997); J.D. Pelletier, *J. Clim.* **10**, 1331 (1997); J.D. Pelletier and D.L. Turcotte, *Adv. Geophys.* **40**, 91 (1999).  
 [17] P. Talkner and R.O. Weber, *Phys. Rev. E* **62**, 150 (2000); *J. Geophys. Res., [Atmos.]* **106**, 20131 (2001).  
 [18] A.-L. Barabasi and H.E. Stanley, *Fractal Concepts in Surface Growth* (Cambridge University Press, Cambridge, 1995).  
 [19] J. Feder, *Fractals* (Plenum, New York, 1989).  
 [20] D.L. Turcotte, *Fractals and Chaos in Geology and Geophysics* (Cambridge University Press, Cambridge, 1992).  
 [21] S. Lovejoy and D. Schertzer, *Nonlinear Variability in Geophysics: Scaling and Fractals* (Kluwer Academic Publishers, Dordrecht, MA, 1991); D. Lavalley, S. Lovejoy, and D. Schertzer, in *Fractals in Geography*, edited by L. DeCola and N. Lam (Prentice-Hall, Englewood Cliffs, NJ, 1993), pp. 158–192; G. Pandey, S. Lovejoy, and D. Schertzer, *J. Hydrol.* **208**, 62 (1998).  
 [22] The crossover increases, as an artefact of the DFA method, with increasing order of DFA. DFA0 and DFA1 give the best estimate for the crossover (see also Refs. [9–11]).  
 [23] K. Fraedrich and R. Blender, *Phys. Rev. Lett.* **90**, 108501 (2003).  
 [24] *Climate Change 2001: The Scientific Basis, Contribution of Working Group I to the Third Assessment Report of the Intergovernmental Panel on Climate Change (IPCC)*, edited by J.T. Houghton *et al.* (Cambridge University Press, Cambridge, 2001).